Available online at www.sciencedirect.com
SCIENCE DIRECT®
Nuclear Instruments and Methods in Physics Research A 557 (2006) 87–93
NUCLEAR INSTRUMENTS & METHODS IN PHYSICS RESEARCH Section A
www.elsevier.com/locate/nima

Emittance compensation with dynamically optimized photoelectron beam profiles

J.B. Rosenzweig[a,*], A.M. Cook[a], R.J. England[a], M. Dunning[a], S.G. Anderson[b], Massimo Ferrario[c]

[a]Department of Physics and Astronomy, UCLA, 405 Hilgard Avenue, Los Angeles, CA 90095, USA
[b]Lawrence Livermore National Laboratory, 7000 East Avenue, Livermore, CA 94550, USA
[c]Istituto Nazionale di Fisica Nucleare, Laboratori Nazionale di Frascati, Via E. Fermi 41, Frascati, Rome, Italy

Available online 16 November 2005

Abstract

Much of the theory and experimentation concerning creation of a high-brightness electron beam from a photocathode, and then applying emittance compensation techniques, assumes that one must strive for a uniform density electron beam, having a cylindrical shape. On the other hand, this shape has large nonlinearities in the space-charge field profiles near the beam's longitudinal extrema. These nonlinearities are known to produce both transverse and longitudinal emittance growth. On the other hand, it has recently been shown by Luiten that by illuminating the cathode with an ultra-short laser pulse of appropriate transverse profile, a uniform density, ellipsoidally shaped bunch is dynamically formed, which then has linear space-charge fields in all dimensions inside of the bunch. We study here this process, and its marriage to the standard emittance compensation scenario that is implemented in most recent photoinjectors. It is seen that the two processes are compatible, with simulations indicating a very high brightness beam can be obtained. The robustness of this scheme to systematic errors is examined. Prospects for experimental tests of this scheme are discussed.

PACS: 29.25.Bd; 29.25.Bx; 41.75.Ht

Keywords: Emittance; Brightness; Space-charge; Collective effects; Electron source

1. Introduction

In order to obtain the highest brightness electron beams from photoinjectors, it is most common to rely on the *emittance compensation* process [1]. Optimization of this process demands that the transverse fields be as uniform, and linear (in radius r) as possible. Most of the existing theoretical and experimental studies of emittance compensation have, to that end, assumed use of a uniform density electron beam, having a cylindrical shape. However, this shape produces space-charge fields near the beam head and tail that have pronounced nonlinear dependences on the spatial coordinates. These nonlinearities result in both transverse and longitudinal emittance growth.

It has been known for some time [2], however, that a uniform density distribution having ellipsoidal shape yields space-charge fields that are linear in all dimensions (e.g. $E_x \propto x$, $E_z \propto z$). Under such conditions, it is conceivable that one may obtain essentially emittance-growth-free dynamics. How to produce such a distribution has, until recently, remained an unanswered question. Limborg has discussed schemes for manipulating and shaping the photoinjector drive laser pulse so that it has an ellipsoidal distribution [3]. This scheme gives good results, as it is a refinement of the standard LCLS emittance compensation scenario [4], with an improved beam distribution. On the other hand, implementation of this scheme has serious technical challenges.

In 1997, Serafini proposed the dynamic creation of an ellipsoidal bunch by launching an ultra-short, radially shaped beam [5], which then evolves through longitudinal expansion of differing radii in the beam to achieve the

*Corresponding author. Tel.: +1 310 206 4541; fax: +1 310 206 5251.
E-mail address: rosen@physics.ucla.edu (J.B. Rosenzweig).

0168-9002/$ - see front matter © 2005 Elsevier B.V. All rights reserved.
doi:10.1016/j.nima.2005.10.055

desired longitudinal shape. In this work, a 10 s of femtosecond laser pulse with uniform time profile was assumed, which is not technically feasible—pulses this short are now a routine capability of the photocathode drive lasers, but not with such a restrictive profile. On the other had, it has recently been shown by Luiten et al. [6] that in obtaining the correct final ellipsoidal distribution, there is essentially no requirement on the shape of the initial laser pulse other than it be ultra-short (length τ_l much shorter than eventual beam length after space charge expansion). Thus it is a natural, and technically achievable way of producing an ellipsoidal-shaped, nearly uniform density beam.

As the beam dynamics just after photoemission are qualitatively different in the traditional emittance compensation scenario and in Luiten's scheme, it is not immediately apparent that one may successfully combine the two. We study here this possibility, showing that the marriage of emittance compensation and dynamic creation of the ellipsoidal shaped beam produces results that in many ways are superior to those obtained in state-of-the-art designs. As the bunches that are produced are shorter in such standard cases, very high brightness beam creation will be shown to be possible.

In this paper, we begin with a detailed examination of the longitudinal beam dynamics characteristic of ultra-short pulse operating regime. We then explore, using multiparticle simulations, the conditions under which one may obtain emittance compensation in existing photoinjector experimental setups. Deviations from ideal performance, both from physical effects in or near the cathode, and systematic errors, are discussed. Prospects for experimental tests of this scheme are examined.

2. Longitudinal beam dynamics

In the Serafini-Luiten scheme, the beam profile expands and deforms longitudinally to produce, in the final state, a uniformly filled ellipsoid of charge. In the process, phase space rearrangements occur which degrade the emittances—especially in the longitudinal dimension. In order to understand this process, to specify experimental requirements, and to identify experimental signatures associated with the process, we analyze in the following the dynamics of space-charge-dominated beam expansion. We note that the reconfiguring of charge to produce a uniform density is a ubiquitous process in single-component plasmas, of which beams are a prime example. Thus our analysis borrows methods and conceptual framework from previous work in the context of transverse space-charge [7–9].

We begin by assuming illumination of a photocathode with a laser having a time profile given by the normalized (to unity) function $g(t_0)$, which produces emission up to a radius a. Assuming prompt electron emission, the photocurrent is

$$I(t_0) = Qg(t_0) \tag{1}$$

where Q is the total beam charge, and the emission time is characterized by $g_{\max} \sim \tau^{-1}$. We assume now that $c\tau \ll a$, so that the beam's electric field is predominantly longitudinal.

Ignoring the effects of the cathode image charge, we calculate the longitudinal force on an electron as

$$\begin{aligned} F_z(t_0) &= -eE_0 + 4\pi e\sigma_b(r)\int_0^{t_0} g(\tilde{t}_0)\mathrm{d}\tilde{t}_0 \\ &= -eE_0 + 4\pi e\sigma_b(r)G(t_0) \\ &= -eE_0(1-\alpha(r)G(t_0)). \end{aligned} \tag{2}$$

Here we have defined the function $G(t_0) = \int_0^{t_0} g(\tilde{t}_0)\mathrm{d}\tilde{t}_0$ as the integrated (from beam center), fractional beam charge. We have implicitly assumed that G is only a function of t_0, and can therefore be calculated once and for all at emission. This assumption, that electrons do not overtake each other, is termed *laminar flow*. It was assumed, but not shown to hold, in Refs. [5] and [6] that laminarity holds; here we shall illustrate that it indeed does so. The quantity $\sigma_b(r)$ is the beam surface charge density distribution in r. The maximum field associated with a surface charge is $4\pi\sigma_b$, and so we normalize the value of the space-charge field through $\alpha(r) = 4\pi\sigma_b(r)/E_0$. Luiten et al. [6] have given the condition $\alpha \ll 1$ as a requirement for ignoring image charges; we assume that it is satisfied. As no significant transverse electric fields are present by assumption, we take r as constant.

Under these assumptions we can write the energy of a given electron as

$$\gamma(z, r, t_0) = 1 + \gamma'(r, t_0)z \tag{3}$$

where

$$\begin{aligned} \gamma'(r, t_0) &= \frac{F_z(r, t_0)}{m_e c^2} \\ &= \gamma_0'(1-\alpha(r)G(t_0)) \quad \text{and} \quad \gamma_0' = \frac{|eE_0|}{m_e c^2}. \end{aligned} \tag{4}$$

Given the energy, one may find the velocity, and integrate it to find z as a function of t

$$\begin{aligned} c[t(r, t_0) - t_0] &= \int_0^z \frac{\mathrm{d}\tilde{z}}{\beta(\tilde{z}, r, t_0)} \\ &= \frac{1}{\gamma'(r, t_0)}\int_1^{\gamma(z,r,t_0)} \frac{\gamma\mathrm{d}\gamma}{\sqrt{\gamma^2-1}} \\ &= \frac{1}{\gamma'(r, t_0)}\sqrt{[\gamma'(r, t_0)z]^2 - 2\gamma'(r, t_0)z}. \end{aligned} \tag{5}$$

After the electron is relativistic, the relative longitudinal motion slows to give an asymptotic form of the final time

$$c[t_f(r, t_0)] \cong z + ct_0 + \frac{1}{\gamma'(r, t_0)} - \frac{1}{\gamma_0'}. \tag{6}$$

Eq. (6) may be used to deduce the form of the final beam distribution. Conservation of probability yields that the current expands by the factor $\partial t_0/\partial t_f$, and so the final current density is given by

$$J(r, z, t_f) = \frac{g(t_0)\sigma_b(r)}{\partial t_f/\partial t_0} \tag{7}$$

where under our assumptions, we may write

$$\frac{\partial t_f}{\partial t_0} = 1 + \frac{\gamma_0' \alpha(r)}{c\gamma'^2(t_0)} g(t_0) \approx 1 + \frac{\alpha(r)}{c\gamma_0'} g(t_0). \quad (8)$$

Note that "wave-breaking" or loss of laminarity [9] is given by the condition $\partial t_f/\partial t_0 = 0$, which is not allowed inside of the beam ($g > 0$); the assumption of laminarity is validated. The current density deduced from Eqs. (7) and (8) is

$$J(r, z, t_f) = \frac{g(t_0)\sigma(r)}{1 + (\alpha(r)/c\gamma_0')g(t_0)} \quad (9)$$

which assuming significant expansion ($\alpha(r) \gg c\tau\gamma_0'$), approaches a constant value

$$J(r, z, t_f) \approx \frac{eE_0^2}{4\pi m_e c}. \quad (10)$$

We therefore deduce that the beam density is uniform, inside of certain boundaries. In order to calculate where the beam edges are, we follow the extrema in the longitudinal coordinate (dropping the constant z of the beam centroid)

$$c[t_f(t_{0,\,\mathrm{edge}})] \cong ct_0 + \frac{1}{\gamma'(r, t_{0,\,\mathrm{edge}})} - \frac{1}{\gamma_0'} \approx ct_0 + \frac{\alpha(r)}{2\gamma_0'} \approx \frac{2\pi m_e c^2}{E_0^2}\sigma_b(r). \quad (11)$$

The position of the bunch boundary in t, and therefore in z, is thus proportional to $\sigma_b(r)$. In order to have this boundary be an ellipse in (r, z) one chooses the surface charge density as

$$\sigma_b(r) = \frac{3Q}{2\pi a^2}\left[1 - \left(\frac{r}{a}\right)^2\right]^{1/2} \quad (12)$$

to obtain

$$ct_{f,\,\mathrm{edge}} \cong \frac{3Qm_e c^2}{E_0^2 a^2}\left[1 - \left(\frac{r}{a}\right)^2\right]^{1/2}. \quad (13)$$

Several phenomena that do not occur in a standard geometry ($\sigma_b(r) = $ constant) are apparent from this analysis. First, one has mixing of electrons between slices during the expansion. Because of this, there is an initial fast increase of the longitudinal emittance, which is terminated by the transition of the field direction from predominantly longitudinal to mainly transverse as the beam accelerates. This "missing" region of transverse space-charge also differentiates this scenario—the geometry of the injected beam in the standard configuration has a length much longer than the radius, and transverse space-charge forces assert themselves nearly immediately, within a propagation length approximately equal to the beam radius. In the Serafini–Luiten scheme, pulse length expansion is required, while in the standard scenario it is avoided.

The formalism we have presented above allows calculation of the transient increase in energy spread and longitudinal emittance during the longitudinal-field dominated region of beam propagation. It does not, however, indicate when the transition from longitudinal field domination to transverse occurs. Thus, even though one may predict the longitudinal expansion from our formalism, the continued growth of longitudinal phase space quantities, unaccompanied by significant expansion, cannot be calculated from Eqs. (3) and (4). Simulations must be used to explore these issues, along with the central issue of emittance compensation.

3. Simulations and emittance compensation

We have performed initial UCLA PARMELA [10] simulations to explore the joining the Serafini-Luiten scheme with the optimized emittance compensation working point (pioneered on the LCLS), of the SPARC injector at LNF-Frascati. We assume that the gun (1.6 cell, 2856 MHz) and solenoid are the same, and run in near to the standard conditions. Through trials, we have optimized the launch conditions of the beam. In order to have values of α which do not give excessive image charge effects the beam charge is lowered, and the beam radius is slightly enlarged. In a preliminary optimization, we launch a 0.33 nC beam with an initial longitudinal Gaussian distribution having $\sigma_t = 33$ fs beam, and a radial Gaussian with $\sigma_x = 0.77$ mm (cutoff at $1.8\,\sigma$). The gun is run with peak, on-axis gradient of 120 MV/m, and the beam is launched at 33° forward of crest. This is well forward of the nominal launch phase for a standard bunch, and serves to control the excessive beam energy spread after the gun. The emittance compensation solenoid is run with peak field $B_z = 2700$ G, which is slightly below the standard scenario, as the beam has slightly lower energy exiting the gun. We note that the peak value of α in our case is 0.11, as opposed to 0.42 in the LCLS design.

There is of course an initial transverse growth emittance which occurs during the reconfiguration of the bunch charge near the cathode, and subsequent growth which may occur to the imperfections in the quasi-ellipsoidal distribution that is formed. It is these effects that are addressed by the emittance compensation process. Emittance compensation is accomplished in two steps: the focusing of the beam by the post-gun solenoid, and the matching of the beam in the first traveling wave linac section (3 m long, SLAC-type, 13.5 MV/m average acceleration), which has a 560 G solenoid field overlaid on it.

The formation of the quasi-ellipsoidal bunch is clearly shown in Fig. 1, which displays the bunch (x, z) distribution at a point 133 cm from the cathode, in the drift space after the gun and just preceding initial traveling wave linac section. Here the beam has 6.3 MeV mean energy, and its transverse dynamics are space-charge dominated. Thus one sees clearly the "inflated" ellipsoidal beam shape. As this shape is obtained purely through space-charge effects, the 6-dimensional transverse phase space is indeed close to the ideal Kapchinskii–Vladimirskii distribution [2]. The final bunch length is 1.3 mm full width, corresponding to a peak current of 105 A. Thus even with

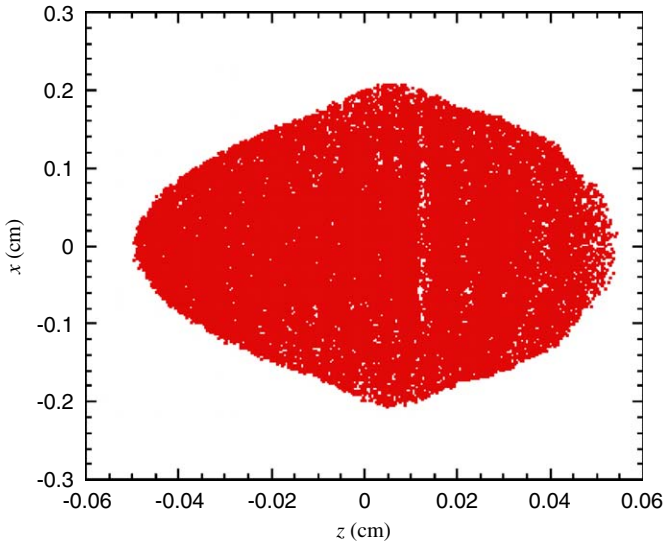

Fig. 1. PARMELA simulation results, showing electron bunch (x, z) distribution 133 cm from cathode (6.3 MeV energy), before injection into the first linac section, showing ellipsoidal beam boundary.

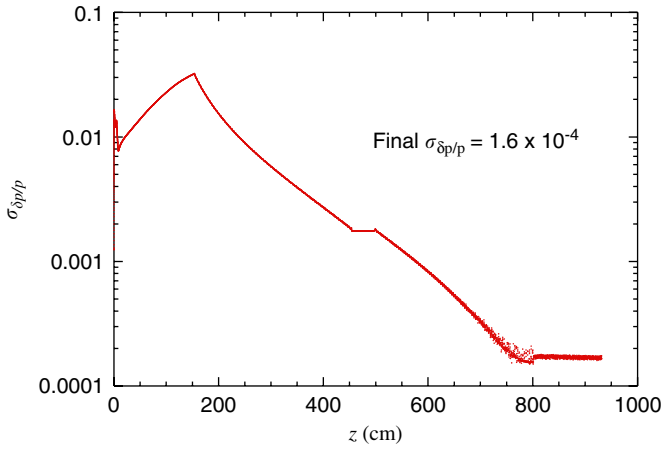

Fig. 2. Evolution of $\sigma_{\delta p/p}$ in z for emittance compensation case, from PARMELA simulation.

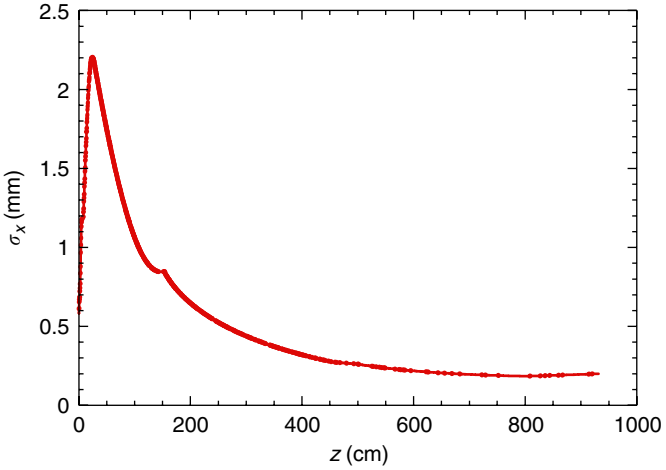

Fig. 3. The evolution of rms transverse beam size σ_x for emittance compensation case, from PARMELA simulation.

one-third of the charge, this scheme should produce a higher current than obtained in simulations of the standard design.

Two notable defects are seen in the beam shape in Fig. 1. The first is the extension of the half-ellipsoid in the trailing part of the bunch as compared with the initial half. This asymmetry is caused by image charge effects. This non-ideal behavior in fact gives the limit on α; when one attempts to launch a higher surface charge density, the bunch deformation from the desired symmetric ellipsoid produces poor emittance performance. The second notable feature is the existence of an anomalous ring at the outer radial edge of the beam. This part of the beam has low surface charge density and experiences radially fringing fields due to its edge location. Because of this, it does not experience enough longitudinal expansion to keep pace with the rest of the bunch, but instead has a moderate amount of radial expansion.

As the longitudinal space-charge during much of the acceleration is also linear, and total pulse length T is short, the longitudinal phase space is very compact. The evolution of the relative momentum spread $\sigma_{\delta p/p}$ in z is shown in Fig. 2. The final achieved rms value is $\sigma_{\delta p/p} = 1.6 \times 10^{-4}$, which is an order of magnitude smaller than that obtained in the standard LCLS-type design.

The evolution of the rms transverse beam size σ_x, and the rms normalized emittance $\varepsilon_{n,\,x}$ are shown in Figs. 3 and 4, respectively. While the behavior of σ_x is similar in most respects to the standard design, with the approximately beam matched at linac entrance to the invariant envelope [1,4], the emittance behavior is not as familiar. In the standard LCLS design, $\varepsilon_{n,\,x}$ achieves a minimum value in the post-gun drift, rising to a local maximum at injection into the linac. The focusing and adiabatic damping of the motion in the linac then produce a monotonic decrease of $\varepsilon_{n,\,x}$ in z. In our case, the transverse space-charge and thus the plasma/emittance oscillations [1] do not "turn on" until after the longitudinal expansion is well underway, thus delaying the emittance minimum in Fig. 4 to occur inside of the linac. In order to produce faster emittance oscillations in the linac to strongly diminish $\varepsilon_{n,\,x}$ before acceleration removes the plasma-dominated beam behavior, the solenoid field in the first linac section has been raised by 40% relative to the standard scenario. This ploy works well, as the final value (still slightly diminishing) of $\varepsilon_{n,\,x}$ at the end of the second linac (84.5 MeV energy) is 0.68 mm mrad. The thermal emittance at the cathode is 0.4 mm mrad, and so the space-charge induced emittance is well compensated.

After acceleration to higher energy (84.5 MeV), the beam is not space-charge dominated, and the (x, z) profile no longer ellipsoidal, as shown in Fig. 5. Nonetheless, the

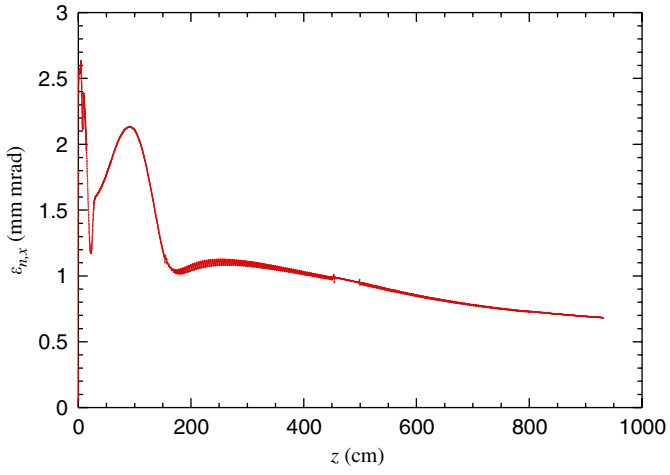

Fig. 4. Evolution of rms normalized emittance $\varepsilon_{n,\ x}$ for emittance compensation case, from PARMELA simulation.

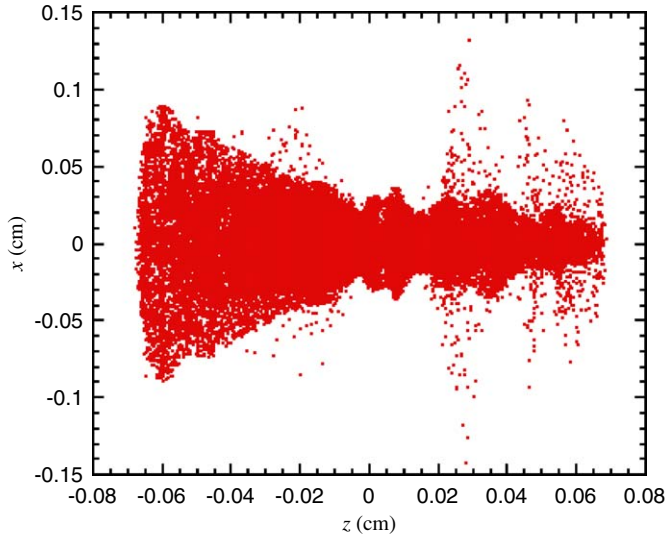

Fig. 5. Electron bunch (x, z) distribution after second linac section (84.5 MeV energy), with ellipsoidal beam shape no longer apparent, from PARMELA simulation.

beam has excellent emittance, and maintains a current profile with shape $I \propto \sqrt{1-(2t/T)^2}$.

With a high initial current, and low intrinsic energy spread, this beam may be compressed further, with very high final peak current achievable. In Fig. 6, we show the resulting longitudinal phase space calculated by a further simulation, using Elegant [11] (with input obtained from PARMELA output), of post-acceleration running forward of crest, and then encountering a chicane. The distribution shown has a final rms bunch length $\sigma_z = 11\,\mu\text{m}$ ($\sigma_t = 37\,\text{fs}$), with a peak current of 4.5 kA. This beam, which has only 0.4% rms momentum spread, has obvious utility in ultra-short pulse FEL or inverse-Compton scattering experiments.

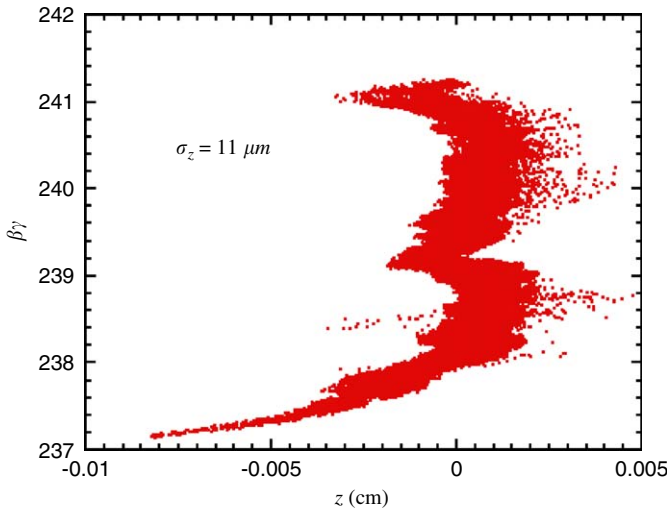

Fig. 6. Longitudinal phase space after third (off-crest) linac section and chicane, showing compression of pulse to $\sigma_z = 11\,\mu\text{m}$, from Elegant/PARMELA simulation.

4. Brightness limits

As the compensation process produces an emittance close to that due to thermal effects at the cathode, the maximum brightness may be calculated for this scheme, which seems to be nearly optimum.

To start, we note that the brightness is given in the simulations case is

$$B_{\max} = \frac{2I}{\varepsilon_n^2} = 5 \times 10^{14}\,\text{A}/(\text{m rad})^2 \tag{14}$$

exceeding that of the LCLS design scheme by a small factor. Using the analysis above as a guide, one may in principle do even better, with

$$B_{\max} = 8\pi J_{\max}\left(\frac{m_e c}{\sigma_{p,x}}\right)^2 \approx \frac{2eE_0^2 m_e c}{\sigma_{p,x}^2} \approx \frac{ecE_0^2}{k_b T_c} \tag{15}$$

where we have used Eq. (10), k_B is the Boltzmann constant, and T_c is the effective cathode temperature. Note the striking scaling that the brightness is now independent of the charge in this regime. For a Mg cathode under illumination by a frequency-tripled Ti:Sapphire laser under the electric fields assumed, $k_B T \cong 0.9\,\text{eV}$, the maximum brightness is deduced to be $B_{\max} \cong 3.75 \times 10^{15}\,\text{A}/(\text{mrad})^2$. This is a factor of 7.5 larger than achieved in the simulations, because: (1) the maximum brightness refers only to the central slice, and so the projected emittance calculated in the simulation provides an over-estimate in the context of Eqs. (14) and (15), (2) the emittance does not reach the thermal limit, and (3) additional pulse lengthening occurs after the gun which is not accounted for in the theoretical analysis. All of these effects may be mitigated,

and one may expect to approach the optimum brightness with further refinements of the scheme.

5. Experimental outlook

Several experimental scenarios are now under investigation, including the PLEIADES injector at LLNL [12], the SPARC injector, and the ORION injector at SLAC [13]. All have the approximately the same gun design (each fabricated at UCLA), and all have traveling wave post acceleration linacs with solenoid focusing overlaid. All of these injectors possess lasers with 100 fs pulse capability, and are adequate for studying the physics of this regime. The PLEIADES injector is not laid out according to the Ferrario optimization, however, and has a non-standard emittance compensation solenoid, as well as a short gun-linac drift distance. The ORION injector is nearly identical to the case studied here, but employs higher gradient X-band linac sections. The SPARC injector is, of course the example we have employed here, and is thus ideal for exploring the physics we have discussed above. This collaboration is now weighing the relative merits of each site.

The experimental signatures that one looks for in tests of this photoinjector operating regime may be delineated. In general terms, the complete emittance compensation scenario presented will show good emittance performance, along with a higher current and short pulse. In addition, at low energy, the beam will have an ellipsoidal shape. This shape may be viewed trivially in z-projection by a standard profile monitor (scintillating crystal, optical transition radiator, etc.). In terms of the longitudinal profile, one may consider use of a streak camera, with an aerogel Cerenkov radiator, to observe the time dependence of the current, and spatially resolve the transverse direction, thus measuring for example, a (x, z) slice of the beam, which should give a uniformly filled ellipse. By scanning this slice in x position, one may reconstruct the entire ellipsoid. Streak cameras may have time resolution as low as 0.25 ps (in practice it may be a bit larger), which is adequate to resolve our beam, which is longer than 4 ps full width. The z-projected transverse phase space (in one dimension) may be investigated at low energy using the multi-slit technique [14].

At higher energy, one may observe the final state of well-compensated emittance through quadrupole scanning [15] or transverse phase space tomography [16]. The ellipsoidal beam in not observable at this energy, as the beam transverse distribution is emittance, and not space-charge dominated, as shown in Fig. 5. The longitudinal distribution can be time-resolved at higher energy at the SPARC injector [17] using a fast RF sweeper [18] with around 30 fs resolution. One may also use longitudinal phase space tomography to observe the higher quality longitudinal phase space. In addition, at SPARC one may use a downstream compressor to investigate compression to the ultra-short bunch length illustrated in Fig. 6. This bunch length presents challenges in measurement, stressing both coherent radiation techniques [19], and RF deflectors.

6. Discussion and conclusions

We have analyzed the feasibility of the marriage between the Serafini-Luiten dynamic beam expansion that produces uniform, ellipsoidally shaped distribution and standard emittance compensation. With some small modifications, it has been seen that they are compatible, and that very high brightness beam performance is obtained in this new scenario. The positive aspects of this proposed operating regime are many. In this scheme, the transverse emittance is found to be quite good, and the longitudinal phase space much improved. One aspect of the quality of the longitudinal phase space is higher current (shorter pulse); another is lower energy spread. Further, the current profile in this regime gives a much improved form of longitudinal wake-fields in addition to the noted improvement in linearity of space-charge forces. These improvements combine to produce a notable improvement in the pulse compression process, mitigating the tendency to produce spikes in the compressed current profile.

Technically, it should noted that the demands on the longitudinal laser pulse-shaping are minimized in comparison with the more standard ''beer-can'' shape previously assumed. The needed pulse widths can be obtained from many of the existing photoinjector drive lasers, which are designed with large bandwidth (short pulse capability) to allow pulse shaping of the flat-top profile with fast rise-small times. Likewise, the transverse pulse shaping is not any more challenging than in the standard case.

Foreseeable drawbacks of this scheme include the limitations imposed by cathode image charges, and large energy spread which is present during the compensation process (cf. Fig. 2). These are design considerations, however, and apparently do not introduce strong constraints on performance. The scheme is, on the other hand, much more dependent on laser fluctuations. Overall laser energy changes directly introduce systematic pulse length variations. Illumination or quantum efficiency non-uniformities will also cause notable degradation in the emittance compensation process in this regime. Perhaps the most serious question in implementing this scheme is the promptness of the photoemission—metals should give fast enough response (a few 100 fs is adequate), but high quantum efficiency semiconductor cathodes are probably not. On a similar note, one may need to be concerned with the peak laser intensity that is demanded on the cathode in this scenario, and choose a laser.

In all, the outlook for implementation of this scheme is quite positive. Direct experimental tests of the relevant physics and technology are expected within the next year, allowing a more definitive judgment on the usefulness of this regime in time for deployment on the high brightness beam injectors for FELs and other light sources.

Acknowledgements

The authors would like to thank Luca Serafini for useful discussions over many years on this subject. This work was performed under the auspices of the US Department of Energy under contract numbers DE-FG-98ER45693 and DE-FG03-92ER40693.

References

[1] L. Serafini, J.B. Rosenzweig, Phys. Rev. E 55 (1997) 7565.
[2] I.M. Kapchinskii, V.V. Vladimirskii, in: Proceedings of the International Conference on High Energy Accelerators, CERN (Scientific Information Service CERN), Geneva, 1959, p. 274.
[3] C. Limborg, these proceedings.
[4] M. Ferrario, J.E. Clendenin, D.T. Palmer, J. Rosenzweig, L. Serafini, in: J. Rosenzweig, L. Serafini (Eds.), The Physics of High Brightness Beams, vol. 534, World Scientific, Singapore, 2000.
[5] L. Serafini, AIP Conf. Proc. 413 (1997) 321.
[6] O.J. Luiten, S.B. van der Geer, M.J. de Loos, F.B. Kiewiet, M.J. van der Wiel, Phys. Rev. Lett. 93 (2004) 094802-1.
[7] O.A. Anderson, Part. Accel. 21 (1987) 197.
[8] I. Hoffman, J. Struckmeier, Part. Accel. 21 (1987) 69.
[9] S.G. Anderson, J.B. Rosenzweig, Phys. Rev. ST Accel. Beams 3 (2000) 094201.
[10] E. Colby, UCLA, PhD Thesis, FERMILAB-THESIS-1997-03, FNAL, 1997.
[11] M. Borland, Computer code ELEGANT, ANL, http://www.aps.anl.gov/asd/oag/oaghome.shtml.
[12] S.G. Anderson, P. Musumeci, J.B. Rosenzweig, W.J. Brown, R.J. England, M. Ferrario, J.S. Jacob, M.C. Thompson, G. Travish, A.M. Tremaine, R. Yoder, Phys. Rev. ST, Accel. Beams 8 (2005) 014401.
[13] D.T. Palmer, et al., in: Proceedings of Particle Accelerator Conference IEEE, 2001, p. 2251.
[14] S.G. Anderson, J.B. Rosenzweig, G.P. Le Sage, J.K. Crane, Phys. Rev. ST Accel. Beams 4 (2001) 014201.
[15] X. Qiu, et al., Phys. Rev. Lett. 76 (1996) 3723.
[16] V. Yakimenko, et al., Phys. Rev. ST Accel. Beams (2003) 122801.
[17] D. Alesini, et al., Nucl. Instr. and Meth. A 528 (2004) 586.
[18] X.J. Wang, in: Proceedings of Part Accelerator Conference IEEE, 1999, p. 229.
[19] A. Murokh, et al., Nucl. Instr. and Meth. A 410 (1998) 549.